Fibrillar Aggregates of the Tumor Suppressor p53 Core Domain[†]

Daniella Ishimaru,[‡] Leonardo R. Andrade,[§] Luciano S. P. Teixeira,[∥] Pablo A. Quesado,[‡] Larissa M. Maiolino,[‡] Priscila M. Lopez,[‡] Yraima Cordeiro,[‡] Lilian T. Costa,[⊥] Wolfgang M. Heckl,[⊥] Gilberto Weissmüller,[∥] Debora Foguel,[‡] and Jerson L. Silva*,[‡]

Departamento de Bioquímica Médica and Centro Nacional de Ressonância Magnética Nuclear, Laboratório de Biomineralização, Instituto de Ciências Biomédicas, and Laboratório de Física Biológica, Instituto de Biofísica Carlos Chagas Filho, Universidade Federal do Rio de Janeiro, 21941-590 Rio de Janeiro, RJ, Brazil, and Institute of Crystallography, Ludwig Maximilians University, Munich, Germany

Received February 7, 2003; Revised Manuscript Received May 13, 2003

ABSTRACT: Alzheimer's disease, Parkinson's disease, cystic fibrosis, prion diseases, and many types of cancer are considered to be protein conformation diseases. Most of them are also known as amyloidogenic diseases due to the occurrence of pathological accumulation of insoluble aggregates with fibrillar conformation. Some neuroblastomas, carcinomas, and myelomas show an abnormal accumulation of the wild-type tumor suppressor protein p53 either in the cytoplasm or in the nucleus of the cell. Here we show that the wild-type p53 core domain (p53C) can form fibrillar aggregates after mild perturbation. Gentle denaturation of p53C by pressure induces fibrillar aggregates, as shown by electron and atomic force microscopies, by binding of thioflavin T, and by circular dichroism. On the other hand, heat denaturation produced granular-shaped aggregates. Annular aggregates similar to those found in the early aggregation stages of α-synuclein and amyloid-β were also observed by atomic force microscopy immediately after pressure treatment. Annular and fibrillar aggregates of p53C were toxic to cells, as shown by MTT [3-(4,5-dimethylthiazol-2-yl)-2,5-diphenyltetrazolium bromide] reduction assay. Interestingly, the hot-spot mutant R248Q underwent similar aggregation behavior when perturbed by pressure or high temperature. Fibrillar aggregates of p53C contribute to the loss of function of p53 and seed the accumulation of conformationally altered protein in some cancerous cells.

Many diseases arise from mutations in proteins, causing loss of their functions, which can be attributed to loss of catalytic activity, loss of structural functions, or even diminished protein stability (*1*). A common feature in these diseases is the altered protein conformation, generating the so-called protein conformation diseases. Protein conformation diseases (PCD's)[1] can be divided into two groups. In the group of diseases known as amyloidosis, large masses of misfolded proteins aggregate in cells of the brain and other organs, causing their destruction (*2*−*6*). Such disorders include Alzheimer's disease, Parkinson's disease, transmissible spongiform encephalopathies, familial amyloid polyneuropathy, Huntington's disease, type II diabetes, and a number of other well-known diseases. In the other group, a small genetic error, usually affecting a single amino acid residue, leads to a misfolded conformation that is either functionally defective or extremely susceptible to cellular proteases (*5*). This group of diseases includes cystic fibrosis, inherited emphysema, and many types of cancer. More recently, it has been demonstrated that some proteins, which are not associated with any known amyloid disease, can aggregate into amyloid-like fibrils under some special conditions (*7*−*9*). Thus it is quite likely that proteins produced by cells involved in the second group of PCD's also exhibit fibrillar behavior.

The tumor suppressor protein p53 is typical of the proteins that go awry in the second group, and it is involved in ∼50% of human cancers. Mutations in its core domain (p53C) affect its stability and/or its ability to bind DNA (*10*−*12*). Amino acid residue Arg^{248} is the amino acid residue that is most frequently mutated in human cancers. Mutations in its codon are the most common mutant in breast, colon, head and neck, lymphoma/leukemia, and skin cancers and the second most frequent in esophageal, gastric, lung, ovarian, and prostate cancers (*13*). Because this residue is essential for the DNA-binding activity of p53 (*14*), its mutants were classified as contact mutants. However, resolution of the $^{1}H-^{15}N$ HSQC

[†] This work was supported by grants from Conselho Nacional de Desenvolvimento Científico e Tecnológico (CNPq), Programa de Núcleos de Excelência (PRONEX), and Fundação de Amparo à Pesquisa no Estado do Rio de Janeiro (FAPERJ) of Brazil to J.L.S. and D.F. and by international grants from the International Centre for Genetic Engineering and Biotechnology (ICGEB) and from the Howard Hughes Medical Institute to J.L.S. L.T.C. is supported by DAAD.

* Corresponding author. Phone: 5521-2562-6756. Fax: 5521-2270-8647. E-mail: jerson@bioqmed.ufrj.br.

[‡] Departamento de Bioquímica Médica and Centro Nacional de Ressonância Magnética Nuclear, Universidade Federal do Rio de Janeiro.

[§] Laboratório de Biomineralização, Instituto de Ciências Biomédicas, Universidade Federal do Rio de Janeiro.

[∥] Laboratório de Física Biológica, Instituto de Biofísica Carlos Chagas Filho, Universidade Federal do Rio de Janeiro.

[⊥] Institute of Crystallography, Ludwig Maximilians University.

[1] Abbreviations: p53C, core domain of the tumor suppressor protein p53; PCD, protein conformation diseases; AFM, atomic force microscopy; TEM, transmission electron microscopy; ThT, thioflavin T; MTT, 3-(4,5-dimethylthiazol-2-yl)-2,5-diphenyltetrazolium bromide; PI3-SH3, bovine phosphatidylinositol 3′-kinase; HypF-N, amino-terminal domain of the *Escherichia coli* HypN-F protein.

10.1021/bi034218k CCC: $25.00
Published on Web 07/08/2003

NMR spectra of the core domain of R248Q mutant (*15*) revealed that it could also be classified as a structural mutant, since the switch from an Arg to a Gln induced conformational changes not only in residues directly related to DNA binding but in other residues located in helix H2, loop L1, and strands S2 and S2′ as well.

Although p53 mutation is the most frequent genetic change observed in human cancers, it is not the only means by which p53 can be inactivated (*12*, *16*, *17*). Cells with wild-type p53 can also have an inactive p53, allowing malignant cells to arise. Impaired wild-type p53 has been described for neuroblastomas, breast cancer, and colon cancer as well as retinoblastoma (*16*, *18*). Moreover, these cancerous cells have an abnormal accumulation of impaired wild-type p53 that form large protein aggregates (*18*). In these cases, wild-type p53 has been reported to accumulate in the cytoplasm and/or the nucleus (*16*). In a recent article, Wolff et al. proposed that cytoplasmic accumulation of p53 in neuroblastoma cells occurs because of a conformational change in p53 (*19*). Even though in all of these studies there seems to be evidence that the protein is aggregated in the cell, the nature of these aggregates remains unclear.

Here, we demonstrate that the core domain of the tumor suppressor protein (p53C) forms fibrillar aggregates rich in β-sheet. Images of atomic force microscopy and transmission electron microscopy provide clear-cut evidence for the formation of typical fibrillar aggregates of p53C when the protein is subjected to mild denaturing conditions. These aggregates are toxic to cells and may be important to the loss of function of p53 in some types of cancer.

EXPERIMENTAL PROCEDURES

Protein Purification. The plasmid pET11a containing the cDNA of the core domain of the tumor suppressor human protein p53 was transformed into *Escherichia coli* strain BL21(DE3). *E. coli* strain BL21(DE3) was grown at 25 °C to an $OD_{600} = 1.0$ before overnight induction at 15 °C with 0.1 mM isopropyl β-D-thiogalactosidase. Purification was performed as previously described (*10*). p53C at 5 μM in 50 mM Tris-HCl, pH 7.2, 150 mM NaCl, 5 mM DTT, and 5% glycerol was used throughout this paper.

Protein Aggregate Production. p53C was exposed to high temperature or pressure. For heat denaturation, samples were incubated at 25 °C, and temperature was increased stepwise to 55 °C. For pressure denaturation, samples were incubated at 37 °C, and pressure was increased stepwise to 2.9 kbar. Both heat and pressure treatments were 6 h long, and images were collected 24 h, 1 week, and 1 month after heat or pressure treatments. For pressure experiments, the high-pressure cell and principles have been described (*20*, *21*); the cell was purchased from ISS (Champaign, IL).

Fluorescence Spectroscopy and Light Scattering Analysis. Intrinsic fluorescence based on tyrosine/tryptophan emission spectra was analyzed in an ISS/K2 spectrofluorometer (ISS, Champaign, IL). Samples were excited at 278 nm, and emission was collected from 295 to 415 nm. Light scattering experiments were performed with excitation and emission wavelengths set at 320 nm.

Transmission Electron Microscopy. The ultrastructure of proteins subjected to high temperature or pressure treatment was analyzed by TEM using negative staining. A drop containing 5 μL of the protein solution was deposited on a Formvar-coated copper grid. Excess solution was removed, and 5 μL of uranyl acetate (2%) was added. After 1 min, the solution was drawn off with a filter paper, and the sample was examined in a Zeiss 900 EM operated at 80 kV.

Atomic Force Microscopy (AFM) Measurements. For contact mode, we have used an AFM built in collaboration with the Ludwig-Maximilians-Universität (Lehrstuhl für Angewandte Physik) in Munich, Germany. Coverslips were glued to magnetic stainless steel punches and mounted in a fluid cell, and scans were performed with a standard silicon nitride tip (Digital Instruments Inc., Santa Barbara, CA) with a 4 μm^2 pyramidal base mounted on a V-shaped cantilever of spring constant 0.06 N/m. Scan rates were approximately 10 μm/s, and scan forces were maintained below 1 nN, which was high enough to achieve good contrast. Tapping mode images were performed in liquid using a commercial Topometrix AFM. Cantilevers (CSC11, MikroMasch) with a nominal spring constant of 0.35 N/m were used with an oscillation frequency of ~35 kHz. Samples were scanned in 50 mM Tris-HCl, pH 7.2, 150 mM NaCl, 5 mM DTT, and 5% glycerol at room temperature.

Thioflavin T Fluorescence and MTT Reduction Assay. Protein aggregates (300 μL) were incubated with 5 μM ThT in 25 mM phosphate buffer, pH 7.0. Fluorescence was recorded on an ISSPC1 spectrofluorometer (ISS, Champaign, IL) immediately after mixing. The excitation wavelength was 440 nm, and emission was collected from 470 to 540 nm. For the MTT reduction assay, protein samples and RAW macrophage cells were processed as previously described (*22*). Briefly, aggregates were incubated in RPMI medium without phenol red and immediately added to a confluent monolayer of RAW macrophage cells. After a 24 h incubation, 10 μL of a MTT stock solution in PBS was added to a final concentration of 0.5 mg/mL. After a 4 h incubation at 37 °C, 100 μL of lysis buffer (20% SDS, 50% *N*,*N*-dimethylformamide, pH 7.4) was added to each well, and samples were incubated at 37 °C for 15 h. Absorbance values of blue formazan were detected at 540 and 590 nm.

Circular Dichroism. Experiments were carried out at least three times. Far-UV spectra were monitored from 200 to 260 nm in a 2 cm quartz cuvette and recorded in a Jasco J-715 spectropolarimeter (Jasco Corp., Tokyo, Japan) at 25 °C.

RESULTS

Folding intermediates that give rise to aggregates can be obtained either by pressure or by heat denaturation. Heat denaturation and the accompanying aggregation have been described for a number of proteins, including p53C (*10*). In Figure 1, we observed that p53C remains relatively stable at physiological temperatures but undergoes denaturation and aggregation above 37 °C as previously demonstrated (*10*). An identical pattern was observed for the hot-spot mutant R248Q, although it showed a greater denaturation and aggregation (Figure 1A). Applying hydrostatic pressure, which has been used extensively to study protein folding, misfolding, and aggregation (*21*, *23*−*28*), elicited a similar behavior: Panels B and C of Figure 1 show the result of pressurizing wild-type p53C up to 2.9 kbar at 37 °C and R248Q up to 2.9 kbar at 25 °C, respectively. Because the R248Q mutant was very unstable at 37 °C, the high-pressure

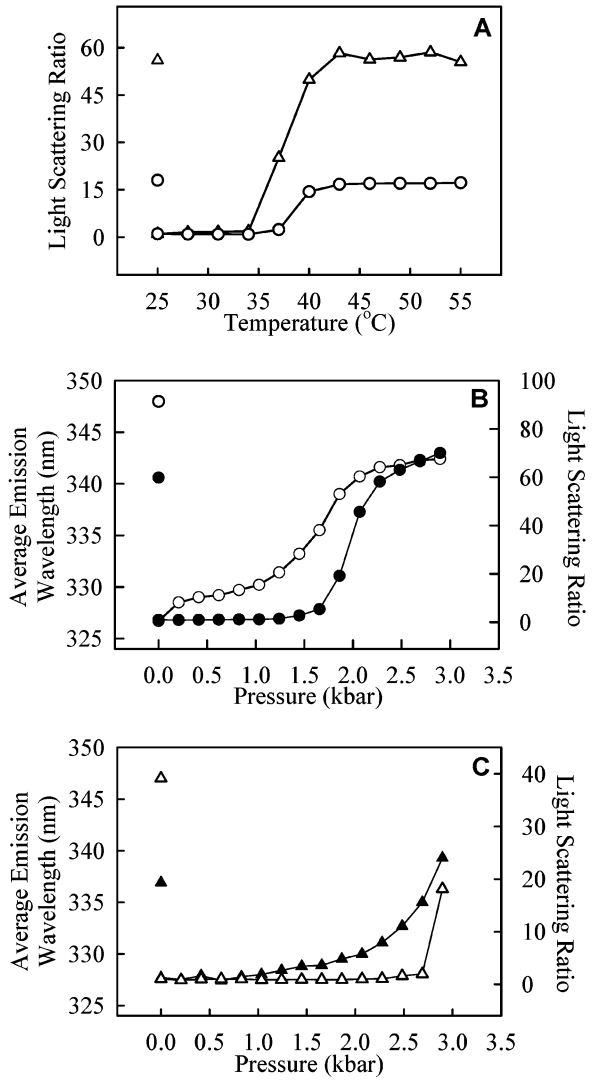

FIGURE 1: Denaturation and aggregation of p53C. Denaturation was monitored by the average emission wavelength of intrinsic fluorescence (closed symbols), and aggregation was measured by light scattering (open symbols). (A) Protein samples were incubated at increasing temperatures to 55 °C: wild-type p53C (circles) and R248Q p53C mutant (triangles). (B, C) Protein samples were pressurized stepwise to 2.9 kbar. (B) Wild-type p53C at 37 °C. (C) R248Q p53C mutant at 25 °C. p53C at 5 μM was used throughout this paper. Other conditions are as described under Experimental Procedures. Isolated symbols at the left correspond to the values of average emission wavelength and light scattering measured after return to 25 °C (A) or after decompression (B, C).

experiments with this mutant had to be performed at 25 °C. Interestingly, wild-type p53C showed a similar behavior to the hot-spot mutant R248Q when subjected to high temperatures and high pressure, with both proteins presenting denaturation associated with aggregation, for heat and pressure treatments. The extent of the aggregation and the structure of the aggregates depend on the final pressure as well as on the temperature.

To characterize the nature of the heat- and pressure-induced aggregates, atomic force microscopy (AFM) and transmission electron microscopy (TEM) were performed (Figure 2). AFM and TEM are standard techniques to analyze protein aggregates (*7*). Heat-induced aggregates had a granular appearance, as demonstrated by AFM and TEM (Figure 2A,B). TEM revealed that these aggregates consisted

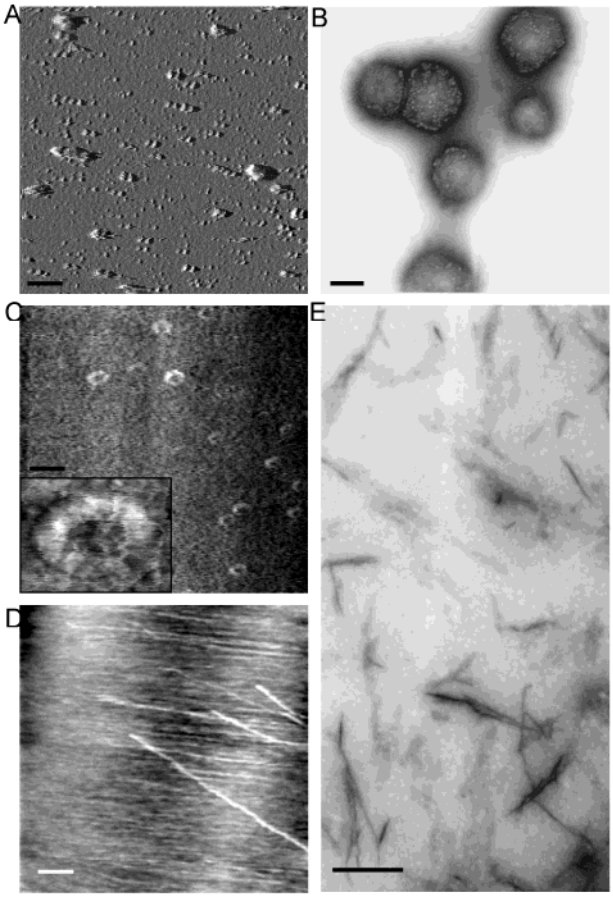

FIGURE 2: Atomic force (AFM) and transmission electron (TEM) microscopy of p53C aggregates. (A, C, D) AFM images of granular aggregates induced by heating (A), annular aggregates induced by pressure (C), both 24 h after treatment, and fibrillar aggregates 1 month after pressure release (D). Calibration bars: 645 nm (A), 240 nm (C), and 265 nm (D). Insert panel shows an original area of 340 × 260 nm. (B, E) TEM images of the samples treated as shown in (A) and (D), respectively, 1 month after heat (B) or pressure (E) treatments. Calibration bars: 320 nm (B) and 240 nm (E).

of large granular spheres (500 ± 70 nm in diameter) with a substructure of smaller ones (Figure 2B). These images were similar 24 h, 1 week, or 1 month after heating the sample. In contrast, pressure-induced aggregates observed by contact mode AFM, 24 h after pressure release (early aggregates), were annular structures of variable sizes (outer diameter, 310 ± 10 nm by 220 ± 20 nm; inner diameter, 130 ± 30 nm by 60 ± 10 nm) (Figure 2C). These particles resemble the amyloid pores described for Alzheimer's Aβ(1−40) "arctic" mutant E22G and Parkinson's α-synuclein A53T and A30P mutants (*6*), except that the ones formed by p53C are much larger. Pressure-induced aggregates older than 1 week or 1 month were not suitable for contact mode AFM imaging. In this case images were acquired by intermittent contact (tapping) mode, revealing large fibers (larger than 1 μm length; 20 ± 5 nm width) (Figure 2D). TEM images from pressure-treated samples 1 week after release of pressure revealed clusters of granular aggregates along with some fibrils (data not shown), while after 1 month aggregates (late aggregates) were very large and visible even to the naked eye. When aggregates from the supernatant of the latter sample were analyzed by TEM (Figure 2E), they appeared as multifibrillar species of variable size (260 ± 60 nm length; 60 ± 3 nm width) with frayed ends, resembling the

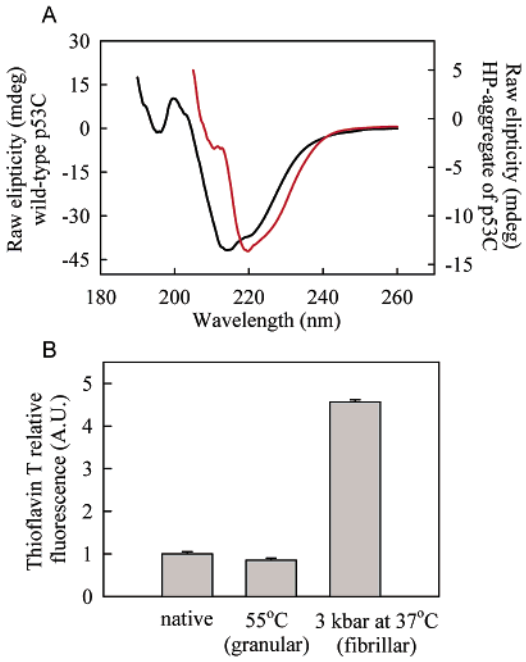

FIGURE 3: Structural properties of p53C aggregates. (A) Far-UV CD spectra of p53C: black line, wild-type p53C; red line, high-pressure-induced fibrillar aggregate. (B) Index of fibrillar structure in pressure- and heat-induced aggregates based on enhancement of thioflavin T fluorescence. The control corresponds to soluble, native protein.

protofibrils from the amino-terminal domain of the *E. coli* HypN-F protein (*22*). Our demonstration of fibrillar aggregates in vitro is consistent with previous reports that show impaired wild-type p53 localized as aggregated structures in both the cytoplasm and nucleus coexisting with diffuse cytoplasmic and/or nuclear p53 (*16*, *18*, *29*). Previously, it was shown that because pressure is a much milder way to denature proteins (*23*−*28*), it gives rise to folding intermediates that can seed amyloid fibrils (*5*).

It has been demonstrated that fibrillar proteins are rich in β-sheet structures (*30*). To assess the secondary structure of p53C fibrils, we used circular dichroism (Figure 3A). Native p53C showed a β-sheet-rich structure, an expected result since estimation of its secondary structure from the primary sequence gives an α-helical content of 8.1% and 46.4% for β-sheet (*31*). The CD spectrum of the p53C fibrillar aggregate revealed the predominance of β-sheet structure with no contribution for α-helix (the ellipticity at 208 nm was close to zero) supporting the fibrillar nature observed for pressure-treated p53C. Pressure-induced formation of fibrils was also investigated by the increase in thioflavin T (ThT) fluorescence (Figure 3B). Thioflavin T is a fluorophore widely used to detect amyloid structure in proteins. In contrast, the nonfibrillar aggregates obtained by heating did not bind thioflavin T to any greater extent than the soluble protein. Thioflavin T usually does not bind to amorphous aggregates.

Protofibrillar aggregates have been suggested to be the toxic, pathogenic species in Alzheimer's disease (*6*) and Parkinson's disease (*32*). In fact, these aggregates as well as amorphous ones have been shown to be cytotoxic in NIH-3T3 cells (*22*). To determine whether p53C aggregates were cytotoxic, we performed assays for cell stress evaluated by MTT [3-(4,5-dimethylthiazol-2-yl)-2,5-diphenyltetrazolium bromide] reduction inhibition assay on RAW mouse macrophage cells (Figure 4). Early aggregates of p53C obtained from high-pressure treatment inhibited MTT reduction by 42.5 ± 3.5%, whereas late, fibrillar aggregates inhibited by 34 ± 1% (bars 3 and 4 in Figure 4). Heat-induced granular aggregates were more toxic (inhibition was 53.5 ± 2.5%). Overall, our data show that the aggregates have different toxicities, with granular being more toxic, followed by the early and late fibrils.

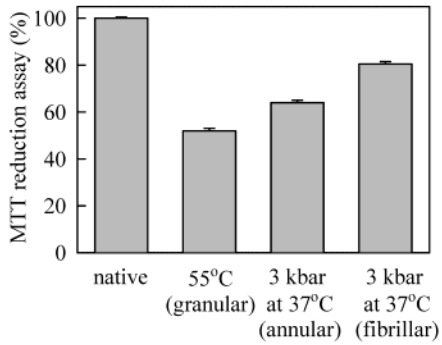

FIGURE 4: Cytotoxicity of p53C aggregates. Toxicity of heat-induced granular aggregates and pressure-induced protofibrillar and fibrillar aggregates. Aggregates were incubated with RAW macrophage cells for 24 h. Cell cultures were incubated with MTT (0.5 mg/mL) for 4 h. Toxicity was evaluated after cell lysis and blue formazan detection at 540 and 590 nm.

DISCUSSION

Although p53 is considered to be typical of the proteins that may go awry and become defective, it has never been shown to make fibrillar aggregates similar to those found in other protein conformation diseases. p53 has been the target most investigated for new anticancer drugs due to the fact that mutation in the *p53* gene is the most frequent genetic change observed in human cancers. However, mutation in both p53 alleles is not the only means by which the protein can be inactivated. Mutation of only one allele can cause p53 inactivation to occur, as a result of the dominant-negative effect (*33*, *34*). In this case, mutant forms of p53 drive the wild-type protein into an inactive, mutant conformation by heterotetramerization. In other words, some mutants are able to replicate their inactive structural information. In fact, most p53 point mutants have been shown to have different degrees of negative dominance (*35*). Cancer cells with mutant p53 have been described to accumulate p53 (*36*). It has been demonstrated that several p53 mutants, including the most frequent ones (also known as hot-spot mutants), have lower protein stability than the wild-type protein (*10*, *12*, *37*). This result suggests that the accumulated mutant protein believed to represent p53 with higher stability may in fact represent less stable forms of the protein. Therefore, the status of the accumulated mutant protein remains unsolved. In addition, cancer cells containing only wild-type p53 have also been described to accumulate protein (*16*, *18*). Interestingly, in these cases, p53 has been described to form not only punctuate structures in the cytoplasm and/or the nucleus of the cells but also aggregates. Here we report for the first time that the core domain of p53 may form amyloid-like fibrils, rich in β-sheet. The fibrils are very similar to those found with proteins related to amyloidogenic diseases.

Aggregates have been described for a variety of proteins, regardless of their relationship to disease states (*2*, *3*, *9*, *10*,

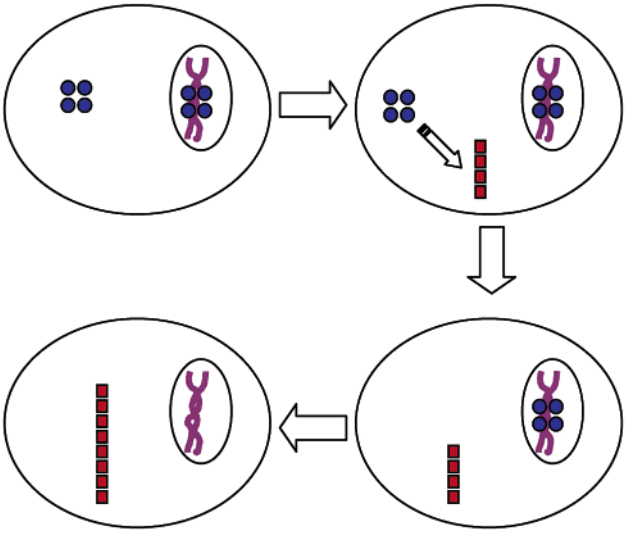

FIGURE 5: Model for p53C aggregation. Model for the conversion of native, active p53 (blue circles) into aggregates (red squares) in the cytoplasm (upper panels). Proteins exported from the nucleus would also be directed into aggregates ensuing loss of the active protein (lower panels). Nuclear DNA is represented in purple.

21, *22*, *25*). Even myoglobin, an α-helical protein, can undergo aggregation into *β*-sheet fibrils under certain conditions (including high pressure) (*9*, *25*). It has been proposed that aggregation is not a random process but one that occurs through specific pathways (*38*, *39*). Significant advances toward the understanding of protein aggregates related to human diseases have been made by the achievement of partially folded intermediates, and pioneer studies were crucial to the idea that protein aggregates contain specific interactions contributing to the polymerization of these partially folding intermediates (*40*, *41*). Here, we took advantage of the fact that high pressure allows one to investigate partially folded intermediates (*27*). The biological relevance of partially folded conformations may lie in the fact that 75% of p53 mutations are point mutations; in other words, the majority of p53 mutants have the full-length protein with a single amino acid substitution and could be seen as alternative conformers of the p53 protein. Our data provide new information regarding the structure of p53C aggregates, raising the possibility that the p53 aggregates already described in cancer cells (*16*, *18*) may represent well-organized structures. Furthermore, irrespective of the structure of these aggregates, we also demonstrated a significant toxicity of aggregates, as has been described for the SH3 domain from bovine phosphatidylinositol 3′-kinase (PI3-SH3) and the amino-terminal domain of the *E. coli* HypN-F protein (HypF-N) (*22*). It has been described that protein aggregates in mammalian cells can occur independently of inclusion-body formation and may form foci (*38*). Although aggregation is generally specific, reflecting precise interactions between partially folded intermediates, other proteins, possibly natural binding partners, can be recruited into an aggregate, providing another mechanism by which protein aggregates disrupt cellular metabolism (*38*). Therefore, a better understanding of how p53 aggregates are formed would be helpful in the search for new anticancer treatments.

In conclusion, in addition to an association with incorrectly folded tumor suppressor protein p53, the pathogenesis of cancer may involve the aggregation of the wrongly folded conformation into fibrils. Besides forming inactive tetramers (*33*, *42*), aggregation could act as a sink to sequester native protein into the inactive conformation, replicating this structural information, as depicted in Figure 5. Hot-spot mutations of p53C, related to highly malignant tumors, usually destabilize the folded conformation (*10*, *12*, *37*), exposing hydrophobic surfaces and presenting a greater tendency to aggregate (Figure 1B). This aggregation is likely to include wild-type subunits (*12*), as has been described for dominant-negative p53 mutants (*33*, *42*). Moreover, p53 has been proposed to belong to the family of loosely folded or partially unstructured native proteins (*43*), which might explain the adoption of mutant-like conformations by the wild-type protein under physiological conditions (*44*). The toxicity of the aggregates of misfolded p53 shown here suggests one more level by which cancer cells can be compromised. One can envisage a gene therapy to combat the conversion of p53 into the inactive and aggregated conformation based on use of a trans-suppressor strategy, as proposed for transthyretin familial amyloid polyneuropathy (*45*). A more stable variant of p53 would shift the equilibrium toward the soluble and active form of the protein (*12*). For several amyloidogenic diseases such as Parkinson's, the early steps of fibrillar formation appear to play a role in the oncogenic process. p53C may provide another example of this route to cellular destruction.

ACKNOWLEDGMENT

We are grateful to Drs. Jonathan King and Martha M. Sorenson for critical reading of the manuscript and Emerson R. Gonçalves for competent technical assistance. We thank Professor H. E. Gaub for the collaboration that allowed us to build an AFM.

REFERENCES

1. Fersht, A. R. (1999) in *Structure and mechanism in protein science. A guide to enzyme catalysis and protein folding* (Fersht, A. R., Ed.) pp 508−539, W. H. Freeman, New York.
2. Dobson, C. M. (1999) Protein misfolding, evolution and disease, *Trends Biochem. Sci. 24*, 329−332.
3. Sacchettini, J. C., and Kelly, J. W. (2002) Therapeutic strategies for human amyloid diseases, *Nat. Rev. Drug Discov. 1*, 267−275.
4. Ellis, R. J., and Pinheiro, T. J. T. (2002) Medicine: Danger—misfolding proteins, *Nature 416*, 483−484.
5. Horwich, A. (2002) Protein aggregation in disease: a role for folding intermediates forming specific multimeric interactions, *J. Clin. Invest. 110*, 1221−1232.
6. Lashuel, H. A., Hartley, D., Petre, B. M., Walz, T., and Lansbury, P. T., Jr. (2002) Neurodegenerative disease: Amyloid pores from pathogenic mutations, *Nature 418*, 291.
7. Chamberlain, A. K., MacPhee, C. E., Zurdo, J., Morozova-Roche, L. A., Hill, H. A. O., Dobson, C. M., and Davis, J. J. (2000) Ultrastructural organization of amyloid fibrils by atomic force microscopy, *Biophys. J. 79*, 3282−3293.
8. Chiti, F., Bucciantini, M., Capanni, C., Taddei, N., Dobson, C. M., and Stefani, M. (2001) Solution conditions can promote formation of either amyloid protofilaments or mature fibrils from the HypF N-terminal domain, *Protein Sci. 10*, 2541−2547.
9. Fändrich, M., Fletcher, M. A., and Dobson, C. M. (2001) Amyloid fibrils from muscle myoglobin, *Nature 410*, 165−166.
10. Bullock, A. N., Henckel, J., DeDecker, B. S., Johnson, C. M., Nikolova, P. V., Proctor, M. R., Lane, D. P., and Fersht, A. R. (1997) Thermodynamic stability of wild-type and mutant p53 core domain, *Proc. Natl. Acad. Sci. U.S.A. 94*, 14338−14342.
11. Rüdiger, S., Freund, S. M. V., Veprintsev, D. B., and Fersht, A. R. (2002) CRINEPT-TROSY NMR reveals p53 core domain

bound in an unfolded form to the chaperone Hsp90, *Proc. Natl. Acad. Sci. U.S.A. 99*, 11085−11090.
12. Bullock, A. N., and Fersht, A. R. (2001) Rescuing the function of mutant p53, *Nat. Rev. Cancer 1*, 68−76.
13. Olivier, M., Eeles, R., Hollstein, M., Khan, M. A., Harris, C. C., and Hainaut, P. (2002) The IARC TP53 Database: new online mutation analysis and recommendations to users, *Hum. Mutat. 19*, 607−614.
14. Cho, Y., Gorina, S., Jeffrey, P. D., and Pavletich, N. P. (1994) Crystal structure of a p53 tumor suppressor-DNA complex: understanding tumorigenic mutations, *Science 265*, 346−355.
15. Wong, K. B., DeDecker, B. S., Freund, S. M., Proctor, M. R., Bycroft, M., and Fersht, A. R. (1999) Hot-spot mutants of p53 core domain evince characteristic local structural changes, *Proc. Natl. Acad. Sci. U.S.A. 96*, 8438−8442.
16. Moll, U. M., Ostermeyer, A. G., Haladay, R., Winkfield, B., Frazier, M., and Zambetti, G. (1996) Cytoplasmic sequestration of wild-type p53 protein impairs the G1 checkpoint after DNA damage, *Mol. Cell. Biol. 16*, 1126−1137.
17. Gottifredi, V., and Prives, C. (2001) Getting p53 out of the nucleus, *Science 292*, 1851−1852.
18. Ostermeyer, A. G., Runko, E., Winkfield, B., Ahn, B., and Moll, U. M. (1996) Cytoplasmically sequestered wild-type p53 protein in neuroblastoma is relocated to the nucleus by a C-terminal peptide, *Proc. Natl. Acad. Sci. U.S.A. 93*, 15190−15194.
19. Wolff, A., Technau, A., Ihling, C., Technau-Ihling, K., Erber, R., Bosch, F. X., and Brandner, G. (2001) Evidence that wild-type p53 in neuroblastoma cells in a conformation refractory to integration into the transcriptional complex, *Oncogene 20*, 1307−1317.
20. Paladini, A. A., Jr., and Weber, G. (1981) Pressure-induced reversible dissociation of enolase, *Biochemistry 20*, 2587−2593.
21. Ferrão-Gonzales, A. D., Souto, S. O., Silva, J. L., and Foguel, D. (2000) The preaggregated state of an amyloidogenic protein: Hydrostatic pressure converts native transthyretin into the amyloidogenic state, *Proc. Natl. Acad. Sci. U.S.A. 97*, 6445−6450.
22. Bucciantini, M., Giannoni, E., Chiti, F., Baroni, F., Formigli, L., Zurdo, J., Taddei, N., Ramponi, G., Dobson, C. M., and Stefani, M. (2002) Inherent toxicity of aggregates implies a common mechanism for protein misfolding diseases, *Nature 416*, 507−511.
23. Silva, J. L., Silveira, C. F., Correia, A., Jr., and Pontes, L. (1992) Dissociation of a native dimer to a molten globule monomer. Effects of pressure and dilution on the association equilibrium of arc repressor, *J. Mol. Biol. 223*, 545−555.
24. Silva, J. L., and Weber, G. (1993) Pressure stability of proteins, *Annu. Rev. Biochem. 44*, 89−113.
25. Smeller, L., Rubens, P., and Heremans, K. (1999) Pressure effect on the temperature-induced unfolding and tendency to aggregate of myoglobin, *Biochemistry 38*, 3816−3820.
26. St. John, R. J., Carpenter, J. F., Balny, C., and Randolph, T. W. (2001) High-pressure refolding of recombinant human growth hormone from insoluble aggregates. Structural transformations, kinetic barriers, and energetics, *J. Biol. Chem. 276*, 46856−46863.
27. Silva, J. L., Foguel, D., and Royer, C. A. (2001) Pressure provides new insights into protein folding, dynamics and structure, *Trends Biochem. Sci. 26*, 612−618.
28. Lima, L. M., Foguel, D., and Silva, J. L. (2000) DNA tightens the dimeric DNA-binding domain of human papillomavirus E2 protein without changes in volume, *Proc. Natl. Acad. Sci. U.S.A. 97*, 14289−14294.
29. Elledge, R. M., Clark, G. M., Fuqua, S. A., Yu, Y. Y., and Allred, D. C. (1994) p53 protein accumulation detected by five different antibodies: Relationship to prognosis and heat shock protein 70 in breast cancer, *Cancer Res. 54*, 3752−3757.
30. Halverson, K., Fraser, P. E., Kirschner, D. A., and Lansbury, P. T., Jr. (1990) Molecular determinants of amyloid deposition in Alzheimer's disease: conformational studies of synthetic beta-protein fragments, *Biochemistry 29*, 2639−2644.
31. Klein, C., Georges, G., Künkele, K.-P., Huber, R., Engh, R. A., and Hansen, S. (2001) High thermostability and lack of cooperative DNA binding distinguish the p63 core domain from the homologous tumor suppressor p53, *J. Biol. Chem. 276*, 37390−37401.
32. Goldberg, M. S., and Lansbury, P. T. (2000) Is there a cause-and-effect relationship between alpha-synuclein fibrillization and Parkinson's disease?, *Nat. Cell Biol. 2*, E115−E119.
33. Chenè, P. (1998) In vitro analysis of the dominant negative effect of p53 mutants, *J. Mol. Biol. 281*, 205−209.
34. Shaulian, E., Zauberman, A., Ginsberg, D., and Oren, M. (1992) Identification of a minimal transforming domain of p53: negative dominance through abrogation of sequence-specific DNA binding, *Mol. Cell. Biol. 12*, 5581−5592.
35. van Oijen, M. G., and Slootweg, P. J. (2000) Gain-of-function mutations in the tumor suppressor gene p53, *Clin. Cancer Res. 6*, 2138−2145.
36. Prives, C., and Hall, P. A. (1999) The p53 pathway, *J. Pathol. 187*, 112−126.
37. Bullock, A. N., Henckel, J., and Fersht, A. R. (2000) Quantitative analysis of residual folding and DNA binding in mutant p53 core domain: definition of mutant states for rescue in cancer therapy, *Oncogene 19*, 1245−1256.
38. Rajan, R. S., Illing, M. E., Bence, N. F., and Kopito, R. R. (2001) Specificity in intracellular protein aggregation and inclusion body formation, *Proc. Natl. Acad. Sci. U.S.A. 98*, 13060−13065.
39. Wetzel, R. (1994) Mutations and off-pathway aggregation of proteins, *Trends Biotechnol. 12*, 193−198.
40. London, J., Scrzynia, C., and Goldberg, M. E. (1974) Renaturation of *Escherichia coli* tryptophanase after exposure to 8 M urea, *Eur. J. Biochem. 47*, 409−415.
41. Haase-Pettingell, C. A., and King, J. (1988) Formation of aggregates from a thermolabile in vivo folding intermediatein P22 tailspike maturation, *J. Biol. Chem. 263*, 4977−4983.
42. Milner, J., and Medcalf, E. A. (1991) Cotranslation of activated mutant p53 with wild-type drives the wild-type p53 protein into the mutant conformation, *Cell 65*, 765−774.
43. Bell, S., Klein, C., Müller, L., Hansen, S., and Buchner, J. (2002) p53 contains large unstructured regions in its native state, *J. Mol. Biol. 322*, 917−927.
44. Hainaut, P., Rolley, N., Davies, M., and Milner, J. (1995) Modulation by cooper of p53 conformation and sequence-specific DNA binding: role for Cu(II)/Cu(I) redox mechanism, *Oncogene 10*, 27−32.
45. Hammarstrom, P., Schneider, F., and Kelly, J. W. (2001) Trans-suppression of misfolding in an amyloid disease, *Science 293*, 2459−2462.

BI034218K